Energy Efficient Mobility Management for the Macrocell – Femtocell LTE Network

Dionysis Xenakis, Nikos Passas, Ayman Radwan,
Jonathan Rodriguez and Christos Verikoukis

Additional information is available at the end of the chapter

http://dx.doi.org/10.5772/48251

1. Introduction

The demand for higher data rates and improved energy-efficiency have motivated the deployment of short-range, low-cost, consumer-deployed cellular access points, referred to as femtocells [1]. Femtocells are consumer-deployed cellular access points, which interconnect standard user equipment (UE) to the mobile operator network via the end user's broadband access backhaul. Although femtocells typically support up to a few users, e.g., up to four users [2], they embody the functionality of a regular base station which operates in the mobile operator's licensed band. From the mobile operator perspective, the deployment of femtocells reduces the capital and operational costs, i.e., femtocells are deployed and managed by the end user, improves the licensed spectrum spatial reuse, and decongests nearby macrocell base stations. On the other hand, the end users perceive enhanced indoor coverage, improved Quality of Service (QoS), and significant User Equipment (UE) energy savings.

The deployment of femtocells is one of the most promising energy efficiency enablers for future networks [3-5, 23]. The study in [3] indicates that compared to a standard macrocell deployment, femtocell deployments may reduce the energy consumption on both the access network and the mobile terminals from four to eight orders of magnitude. Analogous results are derived in terms of system capacity per energy unit, although the performance degradation due to increased RF interference between the macro – femto and the femto – femto systems is not investigated. The latter effect is incorporated in [4], where it is shown that in-band macro – femto coexistence results in non-negligible performance degradation on the macrocell network layer. Nevertheless, improved QoS and significantly reduced energy consumption per bit are simultaneously achieved in the UE, with respect to the femtocell deployment density. To further reduce the energy consumption on the femtocell access point (FAP), the authors in [5]

INTECH
open science | open minds

© 2012 Xenakis et al., licensee InTech. This is an open access chapter distributed under the terms of the Creative Commons Attribution License (http://creativecommons.org/licenses/by/3.0), which permits unrestricted use, distribution, and reproduction in any medium, provided the original work is properly cited.

propose an idle mode procedure according to which the pilot transmissions are disabled in the absence of nearby cellular user activity. Compared to static pilot transmission, the proposed procedure is shown to significantly reduce the overall signaling overhead due to mobility.

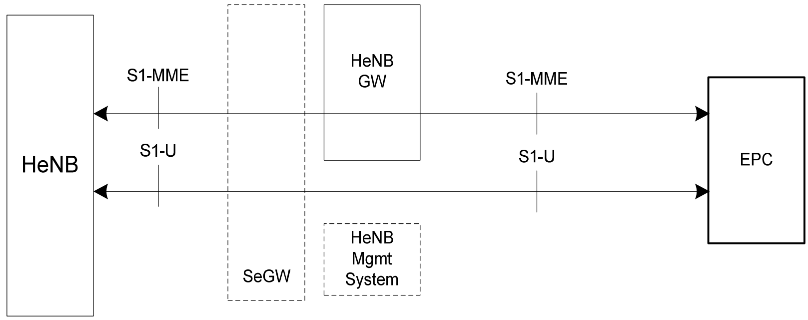

Figure 1. E-UTRAN HeNB Logical Architecture [6]

The Release 9 series of standards for the 3rd Generation Partnership Project (3GPP) the Long Term Evolution (LTE) system [6] is one of the first standards to provision the deployment of femtocells. In the context of LTE, a macrocell is referred to as evolved Node B (eNB), while a femtocell is referred to as Home eNB (HeNB). An LTE user is member of a Closed Subscriber Group (CSG) either if it is permitted to utilize a particular set of closed access femtocells or if it receives prioritized service on a particular set of hybrid access femtocells [7]. The standard describes the cell identification and access control procedures in the presence of LTE femtocells, along with the mobility management procedure for CSG femtocells. Fig. 1 depicts the logical architecture to support femtocells in the LTE system.

As shown in Fig. 2, two of the evolved packet core (EPC) network entities are directly involved in the support of HeNBs, i.e., the Mobility Management Entity (MME) and the Serving Gateway (S-GW). The MME implements the functions of core network (CN) signaling for MM support between 3GPP access networks, idle state mobility handling (e.g. paging), tracking area list management, roaming, bearer control, security, and authentication. On the other hand, the S-GW hosts the functions of lawful interception, charging, accounting, packet routing and forwarding, as well as mobility anchoring for intra and inter-3GPP MM. In the presence of femtocells, the evolved UMTS terrestrial radio access (E-UTRA) air interface architecture consists of eNBs, HeNBs, and HeNB gateways (HeNB GW). The eNBs provide user and control plane protocol terminations towards the UE, and support the functions of radio resource management, admission control, scheduling and transmission of paging messages and broadcast information, measurement configuration for mobility and scheduling, as well as routing of user plane data towards the S-GW. The functions supported by the HeNBs are the same as those supported by the eNBs, while the same implies for the procedures run between the HeNBs and the EPC. The HeNB GW acts as a concentrator for the control plane aiming to support of a large number of HeNBs in a scalable manner. The deployment of HeNB GW is optional; however, if present, it appears to the HeNBs as an MME and to the EPC as an eNB.

The eNBs interconnect with each other through the X2 interface, while they connect to the EPC through the S1 interface [3]. The same implies for the connection between the HeNBs and the EPC, whereas different from the eNB case, the X2 interface between HeNBs is not supported. Fig. 2 illustrates the overall LTE network architecture in the presence of HeNBs.

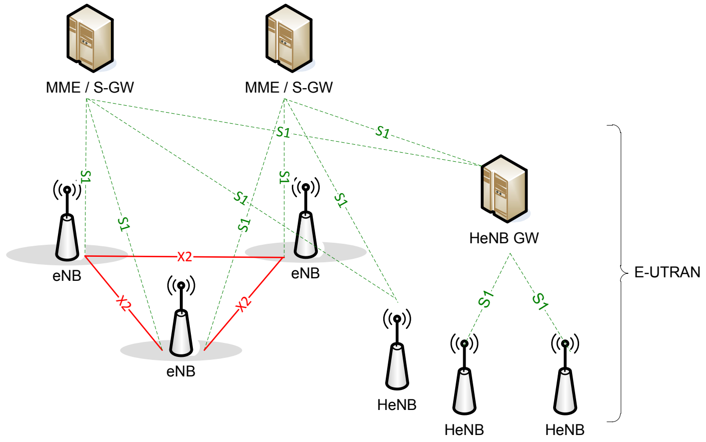

Figure 2. Support of femtocells in the LTE network architecture

In a cellular environment, MM typically consists of three phases [8] a) serving cell monitoring and evaluation, b) cell search and measurement reporting, and c) mobility decision/execution. The serving cell quality is monitored and evaluated on a periodic basis to sustain the service quality over an acceptable threshold. If the service quality falls below a policy-defined threshold, e.g. received signal strength or energy consumption, cell search and measurement reporting is triggered. The cell search and measuring procedure (which bands to sense, in what order, what measurement period and sampling rate to adopt, etc) can be either network-configured or user equipment (UE) based depending on the radio interface standard, the current UE state (e.g. idle or connected), the UE capabilities, and so on. In the former approach, the serving cell exploits its awareness on the surrounding cellular environment to configure the UE to derive and report back signal quality measurements on a predefined set of frequency bands or cells, e.g. provides the UE with a neighbor cell list (NCL) [8]. On the contrary, the UE-based approach is built on the UE capability to autonomously determine when and where to search for neighbor cells without any network intervention. In both cases, a handover (HO) decision entity incorporates the derived signal quality measurements to decide on whether the UE should move to another cell. This entity can reside either on the network (network-controlled approach) or the UE side (mobile-controlled approach) while the decision criteria can incorporate various performance measures such as a) signal quality measures, e.g. received signal strength and SINR, b) user mobility measures, e.g. speed, direction, and c) energy consumption at the UE side, e.g. Joule or Joule/bit. The mobility procedure where the user has no active connections (idle mode) is referred to as cell selection if the user is not camped on a cell or as cell reselection if the user is already camped on a cell. On the other hand, cell HO refers to the mobility procedure performed to seamlessly transfer ongoing user connections from the serving to the target cell (connected mode).

MM in the macrocell – femtocell network comprises many technical challenges in all three phases. Given the femtocell sensitiveness on user mobility and ambient radio frequency (RF) interference, serving cell monitoring and evaluation should be performed in a more frequent basis to sustain an acceptable service quality when connected to a femtocell. Considering the relatively small number of physical cell identifiers in prominent radio air-interfaces, more complicated yet backwards compatible cell identification procedures are required to facilitate cell searching and identification. Furthermore, maintaining and broadcasting a comprehensive Neighbor Cell List (NCL) to facilitate cell search and measurement reporting is not scalable in an integrated femtocell – macrocell network. To this end, novel UE-based cell search procedures are required to fully exploit the underlying femtocell infrastructure. The effectiveness of these procedures will have a great impact on the UE energy autonomicity and perceived QoS as explained in the following.

In the presence of ongoing user connections, cell quality measurements are usually performed during downlink (DL) and uplink (UL) idle periods provided either by Discontinuous Reception (DRX) or by packet scheduling (i.e. gap assisted measurements) [6]. However, the DRX periods are typically utilized for UE energy conservation while the measurement gaps can be utilized to extend the user service time. Taking this into account and considering that a) the short femtocell range results in more frequent cell search and measurement report triggering even under low to medium mobility scenarios, and b) the large number of neighboring cells will substantially increase the aggregated measurement time in dense femtocell deployments, it follows that cell search and measurement reporting may severely deteriorate the user-perceived QoS and deplete the UE battery lifetime. Moreover, searching for and deriving measurements on nearby yet non accessible femtocells should also be avoided, e.g. when a nearby femtocell belongs to a closed access group where the user is not subscribed. In prominent cellular standards, the mobility decision is typically based on signal quality, coverage or load balancing criteria [8, 9]. Given their preferential QoS and significantly reduced energy consumption on the UE side, femtocells are expected to be prioritized over macrocells during the mobility decision phase. However, the mobility decision and execution in an integrated femtocell environment is a non-trivial issue. Femtocell identification introduces non-negligible delay overhead while the limited femtocell capacity in terms of supported users may substantially increase the HO failure probability. The tagged user access status on the candidate femtocells should also be taken into account both to avoid unnecessary signaling overhead and minimize the HO failure probability due to HO rejection [9]. The femtocell sensitiveness on user mobility can substantially increase the number of mobility decision and execution events, increasing thus the network signaling overhead due to mobility management and compromising the UE service continuity when in connected mode.

HO decision affects various aspects of the overall network performance, which mainly include the Signal to Interference plus Noise Ratio (SINR) performance, the interference performance as well as the energy-efficiency at the access network nodes. Current literature includes various HO decision algorithms for the macrocell – femtocell network [10-12], which primarily focus on prioritizing femtocells over macrocells with respect to user

mobility criteria. Emphasis is given in reducing the number of the network-wide HO execution events, owing to the short femtocell radius and the ping-pong effect [9]. Nevertheless, the strongest cell HO decision policy [8] is considered for both macro-macro and femto-femto HO scenarios. According to it, the serving cell proceeds to a HO execution whenever the Reference Signal Received Power (RSRP) [6] of a neighbor cell exceeds over the respective RSRP status of the serving cell plus a policy-defined HHM, for a policy-defined time period namely the Time To Trigger (TTT). The HHM is typically introduced to mitigate UE measurement inconsistencies, encompass frequency-related propagation divergences and minimize the ping-pong effect [9], i.e. consecutive HOs originating from the user movement across the cell boundaries. If comparable downlink Reference Signal (RS) power transmissions are assumed amongst the LTE cells, the strongest cell HO policy facilitates mobility towards a LTE cell with preferential propagation characteristics. However, this is not the case of the macrocell – femtocell LTE network where femtocells are expected to radiate comparably lower downlink RS power for interference mitigation on the macrocell layer [1]. Divergent RS power transmissions are expected even amongst the femtocell layer, in accordance with the adopted self-optimization procedure [5]. Apart from RS power transmission divergences, substantial RF interference divergences are also expected amongst the LTE cells. RF interference is an inevitable product of the unplanned femtocell deployment, both in terms of location and operating frequency, even if advanced interference cancellation and avoidance techniques are adopted [1-2, 14-16]. The RF interference divergences amongst the LTE cells may severely deteriorate the user-perceived QoS due to service outage and substantially increase the network signaling due to mobility, if the interference-agnostic strongest cell HO decision policy is adopted.

In conclusion, apart from improved indoor coverage and enhanced user-perceived QoS, femtocells natively achieve significant energy savings at both the access network and the UE side. To this end, more sophisticated HO decision algorithms are required in the presence of LTE femtocells to fully exploit the native femtocell superiority both in terms of enhanced QoS and reduced energy consumption. The remainder of this chapter discusses an energy-efficient HO decision policy for the macrocell - femtocell LTE network which aims at reducing transmit power at the mobile terminals [17]. The employment of the proposed policy is based on adapting the HO Hysteresis Margin (HHM) with respect to a mean SINR target and standard LTE measurements of the candidate cells' status. The incorporation of the SINR target guarantees QoS, while the utilization of standard LTE measurements provides an accurate estimation of the required UE transmit power per candidate cell. The benefit for employing the proposed HO decision policy is three-fold; improved energy-efficiency at the LTE UEs, lower RF interference, and guaranteed QoS for the ongoing user links. Another important feature of the proposed HO decision policy is that even though it is fundamentally different from the predominant strongest cell HO policy, it is employed in an LTE backwards-compatible manner by suitably adapting the HHM.

The remainder of this chapter is organized as follows. Section 2 models the macrocell – femtocell LTE in network under the viewpoint of MM and discusses the predominant

strongest cell handover decision policy. Section 3 describes the proposed HO decision policy, while section 4 discusses the network signaling procedure required to employ it. Section 5 includes selected simulation results to illustrate its performance in terms of energy consumption per bit, UE power consumption, cell power consumption, and number of HO execution events. Finally, Section 5 concludes the chapter.

2. System model and strongest cell handover decision policy

2.1. System description

A two-tier LTE network is considered, operating within the LTE band set $\boldsymbol{N} \coloneqq \{1, \dots, N\}$. A macrocell station is referred to as evolved Node B (eNB), while a femtocell station as Home eNB (HeNB). To resourcefully sustain its ongoing services, user u is assumed to have a mean SINR target, denoted by $\overline{\gamma}^{u}_{target}$. Let $\boldsymbol{C_n}$ denote the set of LTE cells operating in band $n \epsilon \boldsymbol{N}$, including both eNBs and HeNBs, and $\boldsymbol{U_n}$ the set of users receiving service from an LTE cell within $\boldsymbol{C_n}$. Assuming that user $u \in \boldsymbol{U_n}$ is connected to cell $s \in \boldsymbol{C_n}$, the respective mean uplink SINR for a tagged time interval T is given as follows:

$$\overline{\gamma}^{T}_{u\to s} = \frac{\overline{P}^{T}_{u} \cdot \overline{h}^{T}_{u\to s}}{\sum_{c\in \boldsymbol{C_n}-\{s\}} \overline{P}^{T}_{c} \cdot \overline{h}^{T}_{c\to s} + \sum_{u'\in \boldsymbol{U_n}-\{u\}} \overline{P}^{T}_{u'} \cdot \overline{h}^{T}_{u'\to s} + \left(\overline{\sigma}^{T}_{s}\right)^2} \tag{1}$$

where $\overline{P}^{T}_{u}$ denotes the power transmission of user u, $\overline{h}^{T}_{u\to s}$ the channel gain from user u to cell s, $\overline{P}^{T}_{c}$ the power transmission of cell c, $\overline{h}^{T}_{c\to s}$ the channel gain between cells c and s, and $\overline{\sigma}_s{}^2$ the noise power at cell s, all averaged within the time interval T. Accordingly, the mean downlink SINR is given as follows:

$$\overline{\gamma}^{T}_{s\to u} = \frac{\overline{P}^{T}_{s\to u} \cdot \overline{h}^{T}_{s\to u}}{\sum_{c\in \boldsymbol{C_n}-\{s\}} \overline{P}^{T}_{c} \cdot \overline{h}^{T}_{c\to u} + \sum_{u'\in \boldsymbol{U_n}-\{u\}} \overline{P}^{T}_{u'} \cdot \overline{h}^{T}_{u'\to u} + \left(\overline{\sigma}^{T}_{u}\right)^2} \tag{2}$$

where $\overline{P}^{T}_{s\to u}$ denotes the power transmission of cell s to user u, $\overline{h}^{T}_{s\to u}$ the channel gain from cell s to user u , $\overline{h}^{T}_{u'\to u}$ the channel gain from user $u'$to user u, and $\overline{\sigma}_u{}^2$ the noise power at user u, all averaged within the time interval T.

Let us now focus on the expected UE transmit power for maintaining a link between a tagged user u and cell c. Let $\boldsymbol{L_u} \subseteq \cup_{n \epsilon N} \boldsymbol{C_n}$ indicate the candidate cell set for user u, which consists of accessible LTE cells and has been identified during the network discovery phase. Using Eq. (1) for the mean SINR target $\overline{\gamma}^{u}_{target}$, it can be readily shown that the mean UE power transmissions for maintaining a link between user u and cell $c \in \boldsymbol{L_u}$ can be estimated as follows:

$$\overline{P}^{T}_{u\to c} = \frac{\overline{\gamma}^{u}_{target} \cdot \left(\sum_{c'\in \boldsymbol{C_n}-\{c\}} \overline{P}^{T}_{c'} \cdot \overline{h}^{T}_{c'\to c} + \sum_{u'\in \boldsymbol{U_n}-\{u\}} \overline{P}^{T}_{u'} \cdot \overline{h}^{T}_{u'\to c} + \left(\overline{\sigma}^{T}_{c}\right)^2\right)}{\overline{h}^{T}_{u\to c}} \tag{3}$$

Note that Eq. (3) includes the impact of handing over to cell $c \in \boldsymbol{L_u}$, given that the RF interference caused by the ongoing user link, i.e., $\overline{P}^{T}_{u} \cdot \overline{h}^{T}_{u\to s}$, is not included. Eq. (3) also

corresponds to the UE power consumption, owing to transmit power, for maintaining a link between user u and cell c. The LTE standard describes a wide set of network and UE link quality measurements [18], which can be utilized to estimate the expected SINR in Eq. (1) and (2), and the average UE power transmission in Eq. (3). Table I summarizes standard LTE measurements, and includes the notation followed in this paper for a tagged user u, cell c, and measurement interval T.

Measurement	Definition	Performed by	Notation
Reference signal received power (RSRP)	The linear average over the power contributions (in [W]) of the resource elements that carry cell-specific reference signals within the considered measurement frequency bandwidth. For RSRP determination the cell-specific reference signals R0 shall be used while if the UE may use R1 in addition to R0 if it is reliably detected. The reference point for the RSRP shall be the antenna connector of the UE.	UE	$RSRP_{c\to u}^{T}$
E-UTRA Carrier Received Signal Strength Indicator (RSSI)	The linear average of the total received power (in [W]) observed only in OFDM symbols containing reference symbols for antenna port 0, over $R_{c,DL}$ number of RBs by the UE from all sources, including co-channel serving and non-serving cells, adjacent channel interference, thermal noise etc. RSSI is not reported as a stand-alone measurement rather it is utilized for deriving RSRQ.	UE	$RSSI_{c\to u}^{T}$
Reference Signal Received Quality (RSRQ)	The ratio $R_{c,DL}$×RSRP/(E-UTRA carrier RSSI) where $R_{c,DL}$ is the number of RB's of the E-UTRA carrier RSSI measurement bandwidth. The measurements in the numerator and denominator shall be made over the same set of RBs. The reference point for the RSRQ shall be the antenna connector of the UE.	UE	$RSRQ_{c\to u}^{T}$
Downlink Reference Signal Transmitted Power (DL RS Tx)	The linear average over the power contributions (in [W]) of the resource elements that carry cell-specific reference signals which are transmitted by a tagged cell within its operating system bandwidth. For DL RS TX power determination the cell-specific reference signals R0 and if available R1 can be used. The reference point for the DL RS TX power measurement shall be the TX antenna connector.	E-UTRAN	$P_{c,RS}^{T}$
Received Interference Power	The uplink received interference power, including thermal noise, within the physical RB's bandwidth of N_{sc}^{RB} resource elements. The reported value is averaged over uplink physical RB. The reference point for the measurement shall be the RX antenna connector.	E-UTRAN	$\bar{I}_{c}^{T}$

Table 1. Basic UE and LTE cell measurement capabilities

Note that the $\bar{I}_{c}^{T}$ measurement in Table I corresponds to the linear average of the RIP measurements performed within the tagged cell's operating bandwidth, i.e., the utilized Resource Blocks [19]. To the remainder of this paper, we focus on the HO decision phase,

which is performed in the serving LTE cells. The network discovery procedure is outside the scope of this paper, and it is assumed that for all UEs connected to it, each serving LTE cell has a consistent candidate cell set, and link quality measurements describing its status.

2.2. Strongest cell handover decision policy

In the context of LTE, the strongest cell HO decision policy results in a HO execution whenever the RSRP of an accessible cell exceeds over the RSRP of the serving cell plus a policy-defined HHM, for a policy-defined time period namely the Time To Trigger (TTT) [9]. The HHM is utilized to mitigate frequency-related propagation divergences, and the ping-pong effect. Based on our system model, the strongest cell HO policy for the LTE system is described as follows:

$$\arg\max_{c \in \boldsymbol{L_u}} RSRP^{TTT}_{c\to u,(dB)} \coloneqq \left\{ c \middle| \, RSRP^{TTT}_{c\to u,(dB)} > RSRP^{TTT}_{s\to u,(dB)} + HHM_{c,(dB)} \right\} \quad (4)$$

where $HHM_{c,(dB)}$ corresponds to the HHM for cell $c \in \boldsymbol{L_u}$, and the notation $X_{(dB)}$ to the value of X in decibels (dB). Taking into account the definition of the RSRP in [15], it follows that:

$$RSRP^{T}_{c\to u} = P^{T}_{c,RS} \cdot \overline{h}^{T}_{c\to u} \quad (5)$$

Substituting Eq. (5) to Eq. (4), it follows that the strongest cell policy facilitates mobility towards cells with higher RS power transmissions or improved channel gain. As a result, even though the strongest cell policy may improve the channel gain for the tagged LTE user (Eq. 5), it does not necessarily improves the SINR performance (Eq. 1, 2), given that neither the RF interference, nor the actual RS power transmissions of the target cells, are taken into account. The same implies for the UE power transmissions, which are not necessarily being reduced (Eq. 3) having a negative impact on both the UE power consumption and the RF interference network-wide.

3. The proposed handover decision policy

The proposed HO decision policy, referred to as UE Transmit Power Reduction (UTPR) policy in the following, consists of handing over to the cell with the minimum required UE transmit power, while maintaining the prescribed mean SINR target. The following analysis is pursued to derive the HHM required for minimizing the UE transmit power, based on the available set of standard LTE measurements in Table I. It is assumed that user u receives service from cell s, which has consistent LTE measurements describing the status of every candidate cell $c \in \boldsymbol{L_u}$ for user u, for the time interval $T = TTT$.

Using (5) under the assumption of a symmetric channel gain, the following estimation can be made:

$$\overline{h}^{T}_{u\to c} \cong \overline{h}^{T}_{c\to u} = \frac{RSRP^{T}_{c\to u}}{P^{T}_{c,RS}} \quad (6)$$

By the RIP measurement definition in [18], it follows that:

$$\overline{I}_c^T = \left(\sum_{c' \in \boldsymbol{C_n} - \{c\}} \overline{P}_{c'}^T \cdot \overline{h}_{c' \to c}^T + \sum_{u' \in \boldsymbol{U_n}} \overline{P}_{u'}^T \cdot \overline{h}_{u' \to c}^T + \left(\overline{\sigma}_c^T\right)^2\right) \tag{7}$$

Using Eq. (3), (6), and (7), it can be shown that the UE power transmission on the serving cell s is given by (8).

$$\overline{P}_u^T \triangleq \overline{P}_{u \to s}^T = \frac{\overline{\gamma}_{target}^u \cdot P_{s,RS}^T \cdot \overline{I}_s^T}{RSRP_{s \to u}^T} \tag{8}$$

Following a similar approach, the UE transmit power on the candidate cell c can be estimated as follows:

$$\overline{P}_{u \to c}^T = \frac{\overline{\gamma}_{target}^u \cdot P_{c,RS}^T \cdot \left(\overline{I}_c^T - \overline{P}_u^T \cdot \overline{h}_{u \to c}^T\right)}{RSRP_{c \to u}^T} \tag{9}$$

where the term $\overline{P}_u^T \cdot \overline{h}_{u \to c}^T$ is introduced to include the positive impact of handing over to cell $c \in \boldsymbol{L_u}$, if cells c and s operate in the same LTE band (if not, it is omitted), i.e, if $c, s \in \boldsymbol{C_n}$. Accordingly, handing over to the candidate cell c, is expected to result in reduced UE transmit power compared to the one used in the current serving cell s, if the following are in effect:

$$\overline{P}_{u \to s}^T > \overline{P}_{u \to c}^T \Rightarrow \tag{10}$$

$$\frac{\overline{\gamma}_{target}^u \cdot P_{s,RS}^T \cdot \overline{I}_s^T}{RSRP_{s \to u}^T} > \frac{\overline{\gamma}_{target}^u \cdot P_{c,RS}^T \cdot \left(\overline{I}_c^T - \overline{P}_u^T \cdot \overline{h}_{u \to c}^T\right)}{RSRP_{c \to u}^T} \Rightarrow \tag{11}$$

$$RSRP_{c \to u}^T > RSRP_{s \to u}^T \cdot \frac{P_{c,RS}^T \cdot \left(\overline{I}_c^T - \overline{P}_u^T \cdot \overline{h}_{u \to c}^T\right)}{P_{s,RS}^T \cdot \overline{I}_s^T} \tag{12}$$

where Eq. (11) is derived by using Eq. (8), and (9), and Eq. (12) by rearranging (11). Note that the parameter $\overline{P}_u^T$ is given by Eq. (8). By taking the respective parameter values in dB, Eq. (12) can be rearranged as follows:

$$RSRP_{c \to u,(dB)}^{TTT} > RSRP_{s \to u,(dB)}^{TTT} + HHM_{c,(dB)}^{UTPR} \tag{13}$$

where the parameter $HHM_{c,(dB)}^{UTPR}$ is given by (14).

$$HHM_{c,(dB)}^{UTPR} = \begin{cases} 10\log \dfrac{P_{c,RS}^{TTT} \cdot \left(\overline{I}_c^{TTT} - \overline{P}_u^{TTT} \cdot \overline{h}_{u \to c}^{TTT}\right)}{P_{s,RS}^{TTT} \cdot \overline{I}_s^{TTT}} & c, s \in \boldsymbol{C_n} \\ 10\log \dfrac{P_{c,RS}^{TTT} \cdot \overline{I}_c^{TTT}}{P_{s,RS}^{TTT} \cdot \overline{I}_s^{TTT}} & otherwise \end{cases} \tag{14}$$

It can be seen that Eq. (13) can be utilized as a HO decision criterion for minimizing the UE power transmissions in the two-tier LTE network. To achieve this, Eq. (14) can be incorporated in the standard LTE HO procedure, as an adaptive HHM. Given that a HHM for mitigating the side-effects of user mobility is still required, the $HHM_{c,(dB)}^{UTPR}$ parameter should be incorporated as an additional HHM in the strongest cell HO decision policy. Taking this into account, the proposed UTPR HO decision policy can be described as follows:

$$\arg\max_{c\in \boldsymbol{L_u}} RSRP_{c\to u,(dB)}^{TTT} \coloneqq \left\{c \mid RSRP_{c\to u,(dB)}^{TTT} > RSRP_{s\to u,(dB)}^{TTT} + HHM_{c,(dB)} + HHM_{c,(dB)}^{UTPR}\right\} \quad (15)$$

Summarizing, the proposed UTPR policy is based on standard LTE measurements, while it is employed by introducing an adaptive HHM to the standard LTE HO procedure. The employment of the UTPR policy does not require any enhancements for the LTE UEs, however, an enhanced network signaling procedure is necessitated. Next section provides some insights on how the proposed policy could be employed in the context of the macrocell – femtocell LTE network.

4. Network signaling to employ the proposed handover decision policy

To identify and ultimately utilize CSG femtocells within its proximity, each LTE UE maintains a CSG whitelist. The respective CSG whitelist per LTE user is also maintained in the Mobility Management Entity (MME), residing in the LTE Core Network (CN), in order to perform access control during the mobility execution phase. The closed and hybrid access LTE femtocells broadcast their CSG identity (CSG ID) along with a CSG indicator set to 'TRUE' or 'FALSE', respectively. Both these fields along with the E-UTRAN Cell Global Identifier (ECGI), used for global LTE cell identification, are signaled within the System Information Block Type 1 (SIB1) in the LTE downlink [6]. Although this information is not required during the LTE cell search and measurement phase, it is considered prerequisite during the LTE mobility decision and execution phase. To this end, a cell identification procedure is performed, where the UE is reconfigured to obtain the ECGI of the target LTE cell [6]. In the following, we identify and discuss two different LTE network signaling approaches to facilitate the employment of the proposed UTPR-based HO decision policy.

The employment of the proposed UTPR policy necessitates the incorporation of standardized LTE cell measurements on the tagged user's neighbor cell set, i.e. the downlink RS transmitted power P_{RS}^{c} and Received Interference Power $\boldsymbol{I_c}$, $\forall c \in \boldsymbol{L}_u$. These measurements can be commuted through the S1 interface [6] to the serving LTE cell. The entire HO decision parameter set will be referred to as HO context in the following. Depending on whether the required HO context is reported and maintained in a LTE CN entity or not, e.g. the MME, two different network signaling approaches are identified i.e. the reactive and the proactive [24] In the reactive approach the HO context is obtained on request towards the target LTE cell, while in the proactive approach it is directly obtained on request to the MME. To employ the latter, the LTE cells are required to report their HO context status to the MME on a periodic basis. The reporting periodicity should be MME-configured and adapted according to the HO context request history, the LTE CN status and so on. Assuming that the serving eNB can be either a regular eNB or a HeNB, Fig. 3 and 4 illustrate the detailed network signaling [6] required in the reactive and the proactive HO context derivation approaches, respectively. Without loss of generality, it is considered that the serving and the target cell are connected to the same MME.

The cell search and measurement signaling steps for both approaches, i.e. steps 1-7 in the reactive and steps 5-11 in the proactive, are in accordance with [6]. During these steps, the serving eNB configures the UE to identify an appropriate neighbor cell set and derive

consistent RSRP and RSRQ measurements. Notice that the measurement configuration and reporting phase in LTE is triggered on critical events [20], e.g. when the serving cell RSRP is below a network-configured threshold for a network-configured time period TTT. To facilitate subsequent parameter acquisition, each measurement report includes a measurement timestamp. The proximity configuration and indication signaling in Fig.3 and 4 is utilized for UE-based autonomous HeNB discovery, while the System Information (SI) acquisition and report signaling is required for HeNB identification and access control validation [6]. The serving eNB utilizes the reported UE measurements, sent on critical LTE events, for HO decision triggering (steps 8 in the reactive and 12 in the proactive approach) [21, 22].

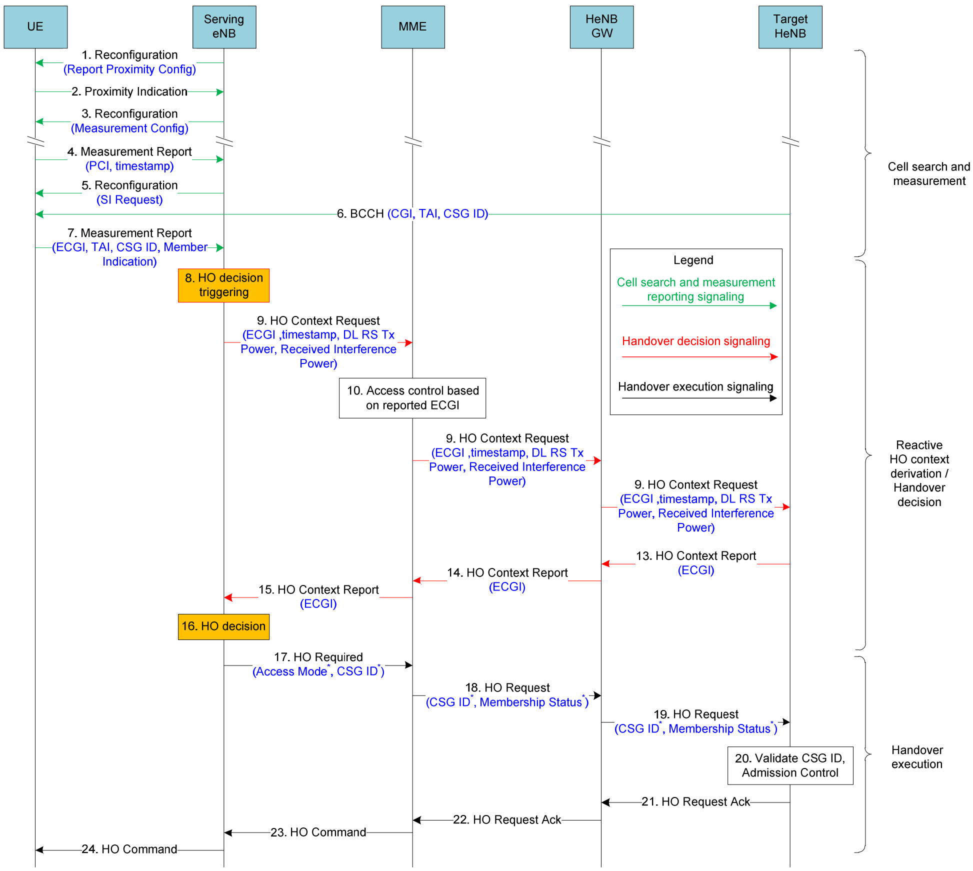

Figure 3. Network signaling procedure for the reactive handover approach

Upon HO decision triggering, the serving eNB initiates a HO context request towards the MME including the corresponding measurement timestamp and target ECGI, i.e. steps 9 in Fig. 3 and 13 in Fig. 4. To minimize unnecessary network signaling, the MME verifies the

access status of the tagged UE on the target ECGI in steps 10 and 14, respectively. If the tagged user is not allowed to access the target eNB, the MME notifies the serving LTE cell accordingly.

The key difference between the reactive and the proactive approaches is that in the former the MME forwards the HO context request towards the target eNB (steps 11-15), while in the latter the MME may directly provide the required HO context by utilizing the reports derived in steps 1-4 (Fig.4). It should be noted that the proactive context derivation signaling phase is indicatively located in steps 1-4, since it can be performed asynchronously with respect to the rest HO signaling procedure. In the absence of HO context close to the required measurement timestamp, the MME may decide to forward the HO context request towards the target eNB as in the reactive approach. Upon HO context acquisition, the HO decision algorithm in the serving eNB proceeds to a HO execution whenever necessary. In that case, a common HO execution signaling follows for both approaches (steps 17-24) [6].

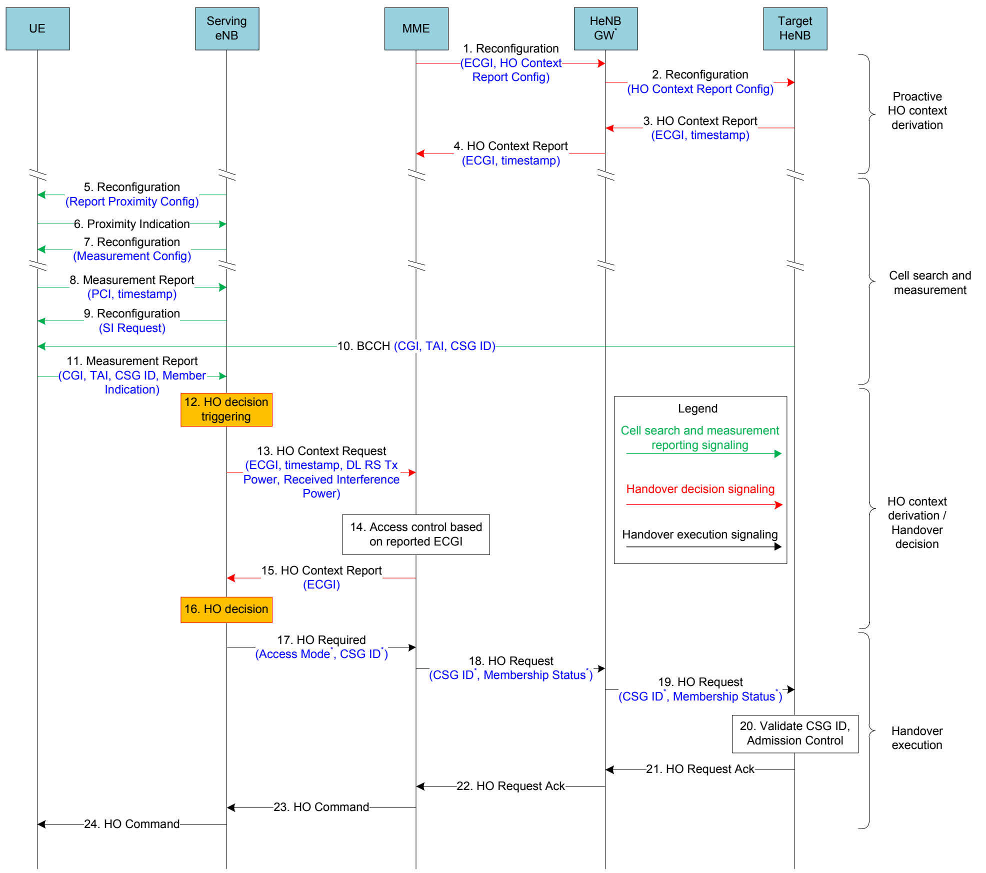

Figure 4. Network signaling procedure for the proactive handover approach

The HO context requests and reports can be signaled in an aggregated manner in both the access (eNB, HeNB) and the core LTE network (MME, HeNB GW). For example, on multiple HO context requests towards a tagged eNB, the MME may send an aggregated HO context request including all the required measurement timestamps. A similar approach can be applied for the HO context report in the reverse direction. Although the reactive approach minimizes the required signaling between the MME and the target LTE cell, the overall network signaling will be highly correlated to the occurrence rate of HO triggering events. On the other hand, more frequent yet more deterministic signaling overhead is expected in the proactive approach, provided that the MME configures the HO context reporting periodicity on the eNBs. In addition to that, the proactive approach may significantly reduce the resulting HO decision delay compared to the reactive approach, provided that the HO context resides on the context-aware MME rather than the target LTE cell. However, certain operational enhancements are required in the MME to resourcefully support the proactive approach, in contrast with the reactive approach where no further LTE CN enhancements are needed.

5. Numerical results

This section includes selected numerical results to evaluate the performance of the proposed UTPR HO decision policy in the macrocell – femtocell LTE network. The simulation scenario is based on the evaluation methodology described in [22], while the proposed HO decision policy is compared against a strongest cell based policy, referred to as SCB policy in the following.

A conventional hexagonal LTE network is considered, including a main LTE cluster composed of 7 LTE cells, where each LTE cell consists of 3 hexagonal sectors. The wrap-around technique is used to extend the LTE network, by copying the main LTE cluster symmetrically on each of the 6 sides. A set of blocks of apartments, referred to as femtoblocks, are uniformly dropped within the main LTE cluster according to the parameter d_{FB}, which indicates the femtoblock deployment density within the main LTE cluster, i.e., the percentage of the main LTE cluster area covered with femtoblocks. Each femtoblock is modeled according to the dual stripe model for dense urban environments in [22]. According to it, each femtoblock consists of two stripes of apartments separated by a 10 m wide street, while each stripe has two rows of $A = 5$ apartments of size 10×10 m. For a tagged femtoblock, femtocells are deployed with a femtocell deployment ratio parameter r_{fc}, which indicates the percentage of apartments with a femtocell [22]. Each femtocell initially serves one associated user, while in general, it can serve up to 4 users. Femtocells and femtocell users are uniformly dropped inside the apartments. Each LTE user is member of up to one CSG, where the CSG ID per user and femtocell is uniformly picked from the set $\{1, 2, 3\}$. Each LTE sector initially serves ten macrocell users, which are uniformly distributed within it. Unless differently stated, it is assumed that $\bar{v} = 3$ km/h and $s_u = 1$ km/h.

The macrocell stations operate in a LTE band centered at 2000MHz, divided into R RBs of width 180 KHz and utilizing a 5MHz bandwidth. The macrocell inter-site distance is set to

500m, while the operating band for each femtocell is uniformly picked from a band set including the macrocell operating band and its two adjacent frequency bands of 5MHz bandwidth. The adopted Modulation and Coding Schemes (MCS) are in accordance with [21], while the Exponential Effective SINR Mapping method is used to obtain the effective SINR per RB and the consequential UE throughput [22]. The minimum required SINR per UE is set to $\overline{\gamma}_t^u$ = 3 dB, while the communications are carried out in full buffer as in [22]. The shadowing standard deviation for the macro and femto systems are 8 and 4 dB respectively, and the macrocell and femtocell noise figures are set to 5 and 8 dB in that order. The macrocell downlink RS power transmissions are normally distributed with a mean value of 23 dBm and a standard deviation of 3dB, while the respective femtocell downlink RS power transmissions are uniformly distributed within the [0,10] dBm interval. The UE power class is set to 23dBm and the maximum transmission powers for the macrocell and femtocell stations are set to 43 and 10dBm [22], respectively. The adopted path loss models are depicted in Table II, where d and d_{indoor} are the total and indoor distances between the tagged cell and the tagged user in meters, respectively. The term $0.7d_{indoor}$ takes into account the penetration losses due to indoor walls, w corresponds to the number of walls separating the UE and the target cell, while L_{ow} = 15 dB and L_{iw} = 5 dB correspond to the penetration losses of the building external and internal walls, respectively. The frequency-selective fading is considered to follow the Rayleigh distribution [8]. Finally, the overall simulation time is set to 200 sec and the simulation unit is set to 1 sec. The key simulation parameters are summarized in Table II.

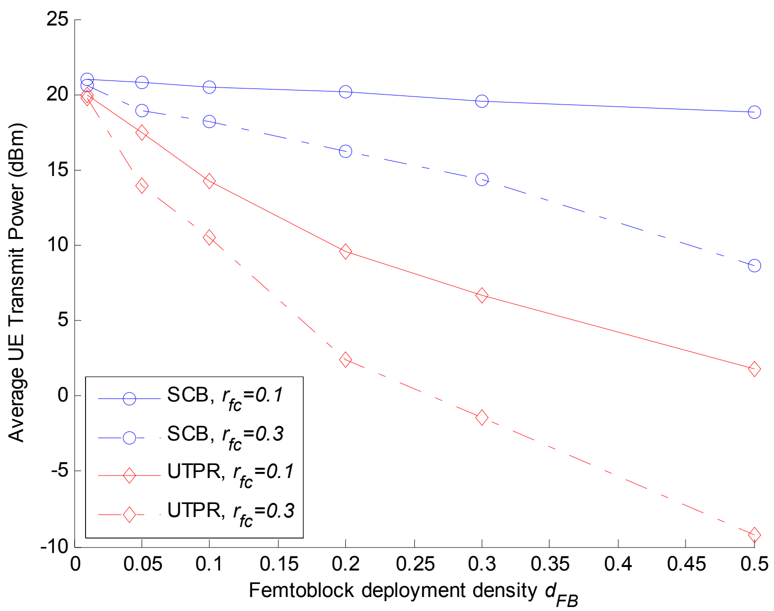

Figure 5. Average UE transmit power versus the d_{FB}

Network layout			
Macrocell layout			7 clusters, 7 sites per cluster, 3 sectors per site, freq. reuse 1
Macrocell inter-site distance			500 m
Initial number of UEs per macrocell sector			10 UEs
Macrocell UE distribution			Uniform within each sector
Femtoblock layout			Dual stripe model for dense urban environments [22]
Femtoblock distribution in the main LTE cluster			Uniform
Femtocell station and UE distribution within an apartment			Uniform
Initial number of UEs per femtocell station			1 UE
Maximum number of supported UE per femtocell			4 UEs
System operating parameters			
Parameter		**Macrocell**	**Femtocell**
Carrier frequency		2000 MHz	Uniformly picked from the set {1990, 2000, 2010} MHz
Channel bandwidth		10 MHz	10 MHz
Maximum Tx Power		$\overline{P}_{max}^{c,T} = 46$ dBm	$\overline{P}_{max}^{c,T} = 20$ dBm
Antenna gain		14 dBi	0 dBi
Noise figure		5 dB	8 dB
Shadowing standard deviation		8 dB	4 dB
RS transmit power (DL RS Tx)		Normally distributed with a mean value of 23 dBm and standard deviation 3dB	Uniformly distributed within the [0,20] dBm interval
CSG ID distribution		Does not apply	Uniform within {1, 2, 3}
Link-to-system mapping		Effective SINR mapping (ESM) [22]	
Path Loss Models			
UE to Macrocell	UE outdoors	$PL(dB) = 15.3 + 37.6log_{10}d$	
	UE indoors	$PL(dB) = 15.3 + 37.6log_{10}d + L_{ow}$	
UE to Femtocell	UE in the same apartment stripe	$PL(dB) = 38.46 + 20log_{10}d + 0.7d_{indoor} + w \cdot L_{iw}$	
	UE outside the apartment stripe	$PL(dB) = \max(15.3 + 37.6log_{10}d, 38.46 + 20log_{10}d) + 0.7d_{indoor} + w \cdot L_{iw} + L_{ow}$	
	UE inside a different apartment stripe	$PL(dB) = \max(15.3 + 37.6log_{10}d, 38.46 + 20log_{10}d) + 0.7d_{indoor} + w \cdot L_{iw} + 2 \cdot L_{ow}$	
Interior / Exterior wall penetration loss (indoor UEs)			5 / 15 dB
UE parameters			
UE power class		$\overline{P}_{max}^{u,T} = 23$ dBm	
UE antenna gain		0 dBi	
Mean UL SINR target		$\overline{\gamma}_t^u = 3$ dB	
CSG ID distribution		Uniformly picked from {1, 2, 3}	
Traffic model		Full buffer similar to [8]	
Mobility model [13]	User speed	$v_t = N(\bar{v}, s_u)$ m/s	
		Mean user speed	$\bar{v} = 3$ km/h
		User speed standard deviation	$s_u = 1$ km/h
	User direction	$\varphi_t = N\left(\varphi_{t-1}, 2\pi - \varphi_{t-1}\tan(\frac{\sqrt{v_t}}{2})\Delta t\right)$	
	where Δt is the time period between two updates of the model, and $N(a, b)$ the Gaussian distribution of mean a and standard deviation b		
Other simulation parameters			
Overall simulation time			200 sec
Simulation time unit			$\Delta t = 1$ sec

Table 2. System-level simulation model and parameters

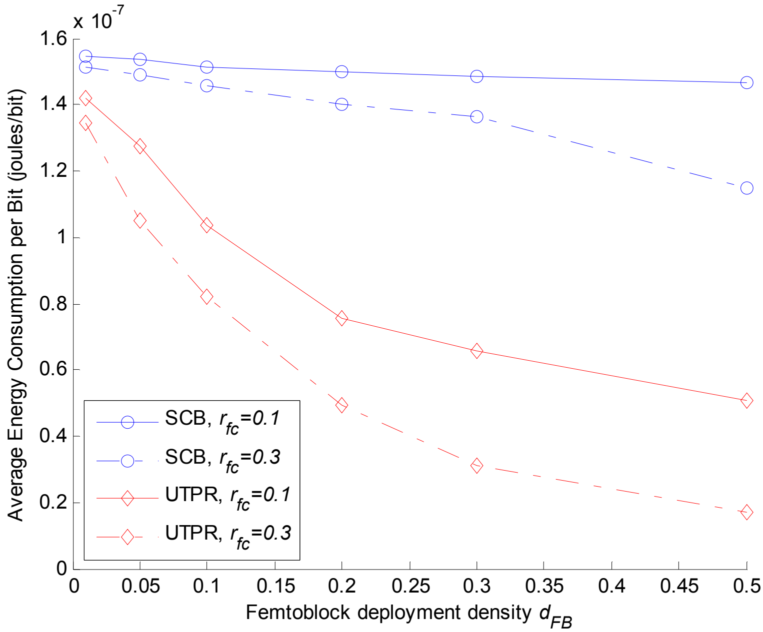

Figure 6. Average UE energy consumption per bit versus the d_{FB}

Fig. 5 and 6 depict the performance of the SCB and UTPR decision policies in terms of UE average transmit power and average energy consumption per bit, owing to transmit power, respectively. Notice that an increased femtoblock deployment density d_{FB} corresponds to an increased number of femtocells and UEs within the main LTE cluster. The same implies for an increased femtocell deployment ratio r_{fc}, which corresponds to an increased femtocell and UE density within each femtoblock. As expected, an increasing femtoblock deployment density d_{FB} or femtocell deployment ratio r_{fc} results in lower UE power and energy consumption per bit for both approaches. However, a higher femtocell deployment ratio r_{fc} is required in order for the SCB policy to benefit from the LTE femtocell presence, both in terms of UE power and energy consumption per bit. On the contrary, the UTPR policy's awareness on the downlink RS and received interference power enables mobility towards LTE cells with lower UE power consumption, while maintaining the tagged user's SINR target. In more detail, for $r_{fc} = 0.1$ and $r_{fc} = 0.3$ the proposed policy results in significantly lower UE power consumption compared to the SCB policy, varying from 1 to 16 dB and 1 to 20 dB respectively. Significantly lower UE energy consumption per bit is also achieved, varying from 10 to 85% compared to the SCB policy, in accordance with the femtoblock deployment density and the femtocell deployment ratio.

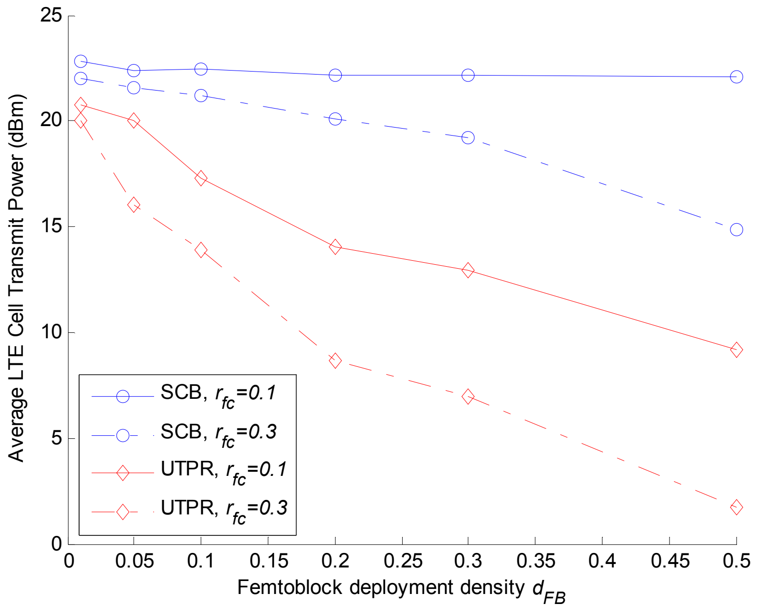

Figure 7. Average LTE cell transmit power versus the d_{FB}

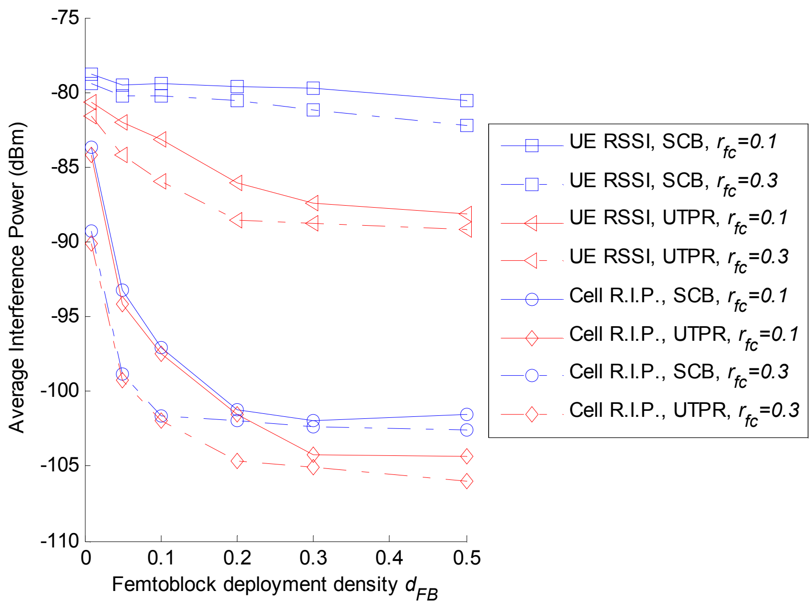

Figure 8. Average UE RSSI and Cell Received Interference Power versus the d_{FB}

The UTPR policy reduces the average transmit power in the LTE cells as well (Fig. 7), as a result of the substantial interference mitigation achieved in the LTE downlink in terms of RSSI and in the LTE uplink in terms of Received Interference Power at the LTE cells (Fig. 8). These are a direct outcome of the proposed policy's tendency to facilitate mobility towards cells which utilize bands with lower Received Interference Power. The latter reduces the number of UE interferers in congested LTE bands and condenses the overall UE power transmissions per band. Although the incorporation of the proposed UTPR policy achieves substantial energy consumption and interference mitigation gains, an increased HO probability is observed compared to the SCB policy (Fig. 9). This follows from the proposed policy's tendency to extend the femtocell utilization time, resulting to an increased sensitiveness on user mobility. To this end, the HO execution events are even more frequent when the femtocell deployment ratio per femtoblock increases. As in the SCB case, standard mobility-centric HO margin $HHM_{c,(dB)}^{UTPR}$ adaptation techniques can be utilized [10-12] to moderate the network-wide number of HO execution events (Fig. 10). The following results are derived for $d_{FB} = 0.05$ and $r_{fc} = 0.2$, while three different mean user speed values are considered i.e. 3, 60 and 125 km/h.

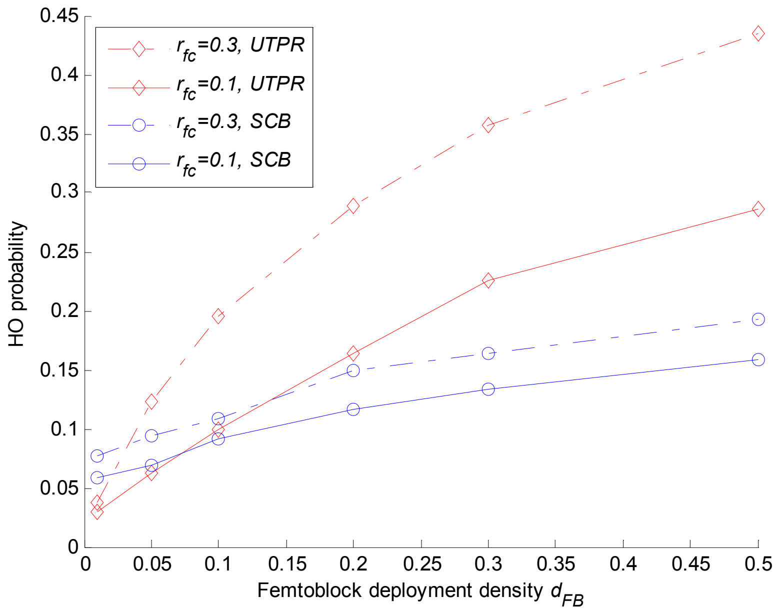

Figure 9. HO probability versus the d_{FB}

Fig. 10 illustrates the HO probability versus the $HHM_{c,(dB)}^{UTPR}$ value. As expected, an increasing user speed raises the HO probability for both policies. However, it can be seen that for a suitable $HHM_{c,(dB)}^{UTPR}$ parameter adaptation, the HO execution events for the UTPR policy are moderated and converge to the number of HO execution events corresponding to the SCB policy with lower $HHM_{c,(dB)}^{UTPR}$ values.

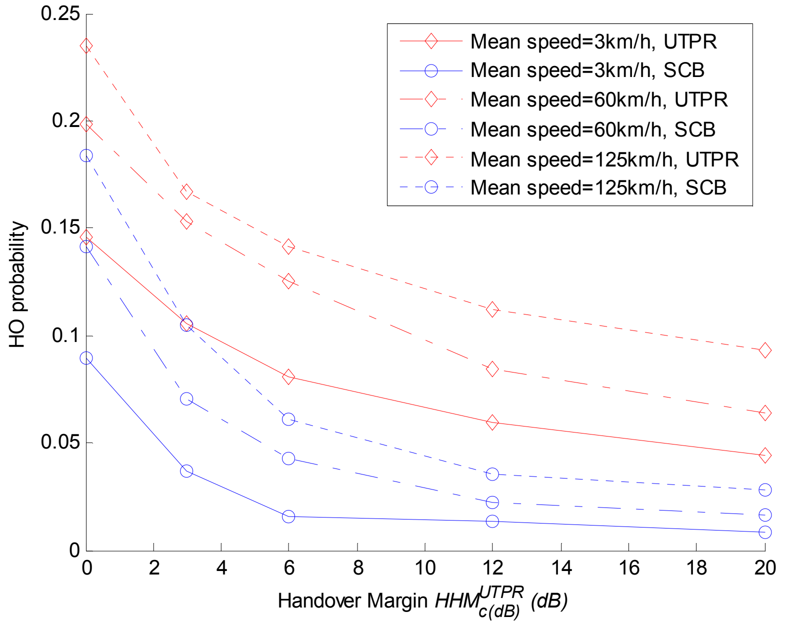

Figure 10. HO probability versus the Handover Margin

6. Conclusion

The random femtocell deployment may result in degraded SINR performance, increased outage probability, and enlarged network signaling, if the interference-agnostic strongest cell policy is employed during the HO decision phase. This chapter discussed the key feature of femtocell deployment and presented a novel HO decision policy for reducing the UE transmit power in the macrocell – femtocell LTE network given a prescribed mean SINR target for the LTE users. This policy is fundamentally different from the strongest cell HO policy, as it takes into account the RS power transmissions and the RF

interference at the LTE cell sites. The proposed policy is backwards compatible with the standard LTE handover decision procedure, as it is employed by adapting the HHM with respect to the user's mean SINR target and standard link quality measurements describing the status of the candidate cells. Even though employing the proposed policy necessitates an enhanced network signaling between cells, numerical results demonstrate greatly lower network-wide RF interference, and reduced UE power consumption owing to transmit power, compared to the strongest cell HO policy. The impact of using an increased HHM for mobility mitigation has also been investigated in terms of HO probability.

Author details

Dionysis Xenakis and Nikos Passas
Dept. of Informatics and Telecommunications, University of Athens, Greece

Ayman Radwan and Jonathan Rodriguez
Instituto de Telecomunicações – Aveiro, Campus Universitário de Santiago, Portugal

Christos Verikoukis
Telecommunications Technological Centre of Catalonia, Barcelona, Spain

Acknowledgement

This paper has been partially funded by the C2POWER (FP7-ICT- 248577) and the GREENET (FP7-PEOPLE 264759), projects, and co-financed by the EU (European Social Fund – ESF) and Greek national funds through the Operational Program "Education and Lifelong Learning" of the National Strategic Reference Framework (NSRF) - Research Funding Program: Heracleitus II. Investing in knowledge society through the European Social Fund.

7. References

[1] V. Chandrasekhar, J. Andrews, A. Gatherer, "Femtocell networks: a survey", IEEE Communications Magazine, vol.46, no.9, pp.59-67, Sept. 2008.
[2] A. Galindo-Serrano, L. Giupponi, M. Dohler, "Cognition and Docition in OFDMA-Based Femtocell Networks," 2010 IEEE Global Telecommunications Conference, pp.1-6, Dec. 2010.
[3] H. Leem, S. Y. Baek, D. K. Sung, "The Effects of Cell Size on Energy Saving, System Capacity, and Per-Energy Capacity," IEEE Wireless Communications and Networking Conference, pp.1-6, Apr. 2010.
[4] F. Cao, Z. Fan, "The tradeoff between energy efficiency and system performance of femtocell deployment," The 7th International Symposium on Wireless Communication Systems (ISWCS), pp.315-319, Sept. 2010.

[5] I. Ashraf, L.T.W. Ho, H. Claussen, "Improving Energy Efficiency of Femtocell Base Stations Via User Activity Detection," IEEE Wireless Communications and Networking Conference 2010, pp.1-5, Apr. 2010

[6] 3GPP, "E-UTRA and E-UTRAN Overall Description.", TS 36.300 V10.1.0 (2010-10)

[7] A. Golaup, M. Mustapha, L.B. Patanapongpibul, "Femtocell access control strategy in UMTS and LTE," IEEE Communications Magazine, vol.47, no.9, pp.117-123, Sept. 2009.

[8] S. Sesia, I. Toufik, M. Baker, "LTE – The UMTS Long Term Evolution: From Theory to Practice", John Wiley & Sons, ISBN: 978-0-470-69716-0, 2009.

[9] K. Dimou, M. Wang, Y. Yang, M. Kazmi, A. Larmo, J. Pettersson, W. Muller, Y. Timner, "Handover within 3GPP LTE: Design Principles and Performance," IEEE 70th Vehicular Technology Conference Fall, pp.1-5, Sept. 2009.

[10] W. Shaohong, Z. Xin, Z. Ruiming, Y. Zhiwei, F. Yinglong, Y. Dacheng, "Handover Study Concerning Mobility in the Two-Hierarchy Network," IEEE 69th Vehicular Technology Conference, pp.1-5, Apr. 2009.

[11] A. Ulvan, R. Bestak, M. Ulvan, "Handover Scenario and Procedure in LTE-based Femtocell Networks", The 4th International Conference on Mobile Ubiquitous Computing, Systems, Services and Technologies, Oct. 2010.

[12] Z. Becvar, P.Mach, "Adaptive Hysteresis Margin for Handover in Femtocell Networks", 6th International Conference on Wireless and Mobile Communications, pp.256-261, Sept. 2010.

[13] J. Zhang, G. de la Roche, "Femtocells : technologies and deployment", John Wiley & Sons Ltd, ISBN 978-0-470-74298-3, 2010.

[14] G. Boudreau, J. Panicker, G. Ning, R. Chang, N. Wang, S. Vrzic, "Interference coordination and cancellation for 4G networks," IEEE Communications Magazine, vol.47, no.4, pp.74-81, Apr. 2009

[15] M. Yavuz, F. Meshkati, S. Nanda, A. Pokhariyal, N. Johnson, B. Raghothaman, A. Richardson, "Interference management and performance analysis of UMTS/HSPA+ femtocells," IEEE Communications Magazine, vol.47, no.9, pp.102-109, Sept. 2009.

[16] O. Simeone, E. Erkip, S. Shamai Shitz, "Robust Transmission and Interference Management For Femtocells with Unreliable Network Access," IEEE Journal on Selected Areas in Communications, vol.28, no.9, pp.1469-1478, Dec. 2010.

[17] D. Xenakis, N. Passas, and C. Verikoukis, "A Novel Handover Decision Policy for Reducing Power Transmissions in the two-tier LTE network", IEEE International Communications Conference (IEEE ICC) 2012, Ottawa, Canada, June 2012.

[18] 3GPP, "Physical layer; Measurements", TS 36.214 V10.0.0 (2010-12)

[19] 3GPP, "LTE physical layer; General description", TS 36.201 V10.1.0 (2010-12)

[20] 3GPP, "Radio Resource Control (RRC); Protocol specification", TS 36.331 V10.0.0.

[21] 3GPP, "User Equipment (UE) radio transmission and reception", TS 36.101 V10.1.0.

[22] Femto Forum, "Interference Management in OFDMA Femtocells", Femto Forum, Mar. 2010.

[23] A. Radwan, J. Rodriguez, "Energy Saving in Multi-standard Mobile Terminals through Short-range Cooperation", EURASIP Journal on Wireless Communications and Networking, to appear.

[24] D. Xenakis, N. Passas, and C. Verikoukis, "An energy-centric handover decision algorithm for the integrated LTE macrocell–femtocell Network", Computer Communications, Elsevier, 2012, to appear. http://dx.doi.org/10.1016/j.comcom.2012.04.024